SF2A 2025
A. Siebert, K. Baillié, M. Béthermin, F. Cantalloube, E. Josselin, N. Lagarde, J. Malzac, J. Richard, L. Selliez, O. Venot (eds)

A BACKWARD MONTE CARLO RADIATIVE TRANSFER MODEL FOR THE TITAN PCM

A. Arfaux[1], S. Vinatier[1], P. Rannou[2], V. Eymet[3], V. Forest[2], Z. He[1], B. Trenquelléon[1], S. Lebonnois[4] and E. Millour[4]

Abstract. We present a comparison of two radiative transfer models in the context of improving the Titan Planetary Climate Model (PCM). In one hand, we have access to the results from the current 2-stream model incorporated in the Titan PCM and in the other hand, we use a 3D backward Monte Carlo model to estimate the heating rates. Our results demonstrate that the sphericity and heterogeneity effects, not accounted with 2-stream models, have major effects on the radiative budget of Titan atmosphere. We conduct this study at equinoxe and solstice, demonstrating the radiative effects of various phenomenon.

Keywords: Titan, GCM, 3D, radiative transfer, Monte Carlo

1 Introduction

Radiative transfer is a major component of Global Climate Models (GCMs), strongly coupled with the dynamic and implemented physical processes (e.g. de Batz de Trenquelléon et al. 2025b). The radiative transfer affects the dynamic of the atmosphere which, in turn, impacts the chemistry as well as the haze and cloud microphysics. The radiation field also directly affects the photochemistry while the produced temperature changes affect directly the chemistry and cloud formation, but also the growth of haze particles. These changes in the chemistry and particles properties exert a feedback on the atmosphere optical properties and then on the radiative transfer. It is therefore of a crucial importance to correctly account for the radiative tranfer in GCMs.

Currently, most GCMs use a 1D plane-parallel radiative transfer model (Lora et al. 2015; de Batz de Trenquelléon et al. 2025b), therefore not accounting for sphericity effects, which might be important in the case of Titan with its thick atmosphere that represents more than a third of its size (with an exobase located at $\sim$ 1500 km above the surface for a body solid radius of 2575 km). Furthermore, the model is applied on independent vertical columns, and misses effects related to horizontal heterogeneities. In addition, the plane-parallel model does not calculate the heating rates in the the polar night region, even at high altitude where the columns are actually illuminated.

To address these limitations, we propose to use a 3D backward Monte Carlo radiative transfer model to evalulate the radiative heating and cooling rates in Titan atmosphere, and we compare the results with those obtained by the 2-stream model used in the Titan Planetary Climate Model (Titan PCM), mainly developped at LMD (Hourdin et al. (1995); Lebonnois et al. (2012); de Batz de Trenquelléon et al. (2025a,b)).

2 Model description

We use hrtdr-planets (`https://www.meso-star.com/projects/htrdr/htrdr.html`, He et al. submitted), a 3D Monte Carlo radiative transfer model developped by Méso-Star, which uses a backward ray tracing algorithm,

[1] LIRA, Observatoire de Paris, Université PSL, CNRS, Sorbonne Université, Université Paris Cité, 5 place Jules Janssen, 92195 Meudon, France
[2] Université de Reims Champagne-Ardenne, CNRS, GSMA, Reims, France
[3] Méso-Star, Toulouse, France
[4] Laboratoire de Météorologie Dynamique (LMD/IPSL), Sorbonne Université, ENS, PSL Research University, Ecole Polytechnique, IP Paris, CNRS, 4 Place Jussieu, 75252 Paris Cedex 05, France

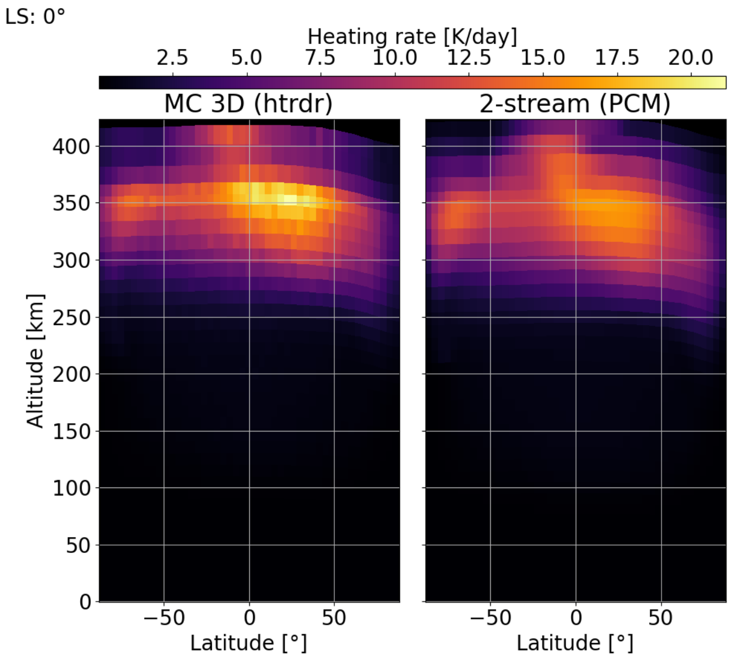

Fig. 1. Heating rates along altitude and latitude, in Titan atmosphere, at equinoxe ($L_S = 0°$), using Titan PCM optical properties. **Left:** Calculation by the 3D Monte Carlo model. **Right:** Calculation by the 2-stream model of the Titan PCM.

incorporating recent developments in computing science such as a null-collision algorithm (Villefranque et al. 2019). In this section, we provide a simplified view of the model algorithm. The rays are launched from the probing point, that is where we aim at evaluating the flux divergence, and the simplified algorithm goes as follows:

- First, a wavelength λ_i is sampled within the range of wavelength we are integrating.
- The ray propagates in the atmosphere in a straight line along a sampled direction, by a distance sampled according to the medium optical properties.
- At the end of this path, an interaction event (often referred as collision) occurs, which can be an absorption, a scattering or a null-collision.
  - In the first case, the ray is terminated and we recover the associated Monte Carlo weight.
  - In the second case, a new direction is sampled according to the local scattering phase function. In this scenario, a direct contribution of the source is evaluated by tracing a new ray in the solar cone and added to the Monte Carlo weight of the original ray. If this new ray reaches the source, the Monte Carlo weight to take into account is the radiance of the source, if it undergoes an absorption, it is zero.
  - In the third scenario, the ray keeps going in the same direction.
- The ray tracing follows, repeating the processes described above until the ray reaches an absorption or leaves the scene.

The Monte Carlo estimate of the flux divergence is obtained by the average of the differences between the Monte Carlo weights w_i brought back by the rays (corresponding to an evaluation of the radiance received at the probing point $\vec{r}$) and the local Planck emission of the atmosphere $B(T, \lambda)$ at temperature $T(\vec{r})$, multiplied by the absorption coefficient k_a:

$$\vec{\nabla}\vec{F}(\vec{r}) = \frac{1}{N}\sum_{i=1}^{N} k_a(\vec{r}, \lambda_i)\,(w_i - B(T(\vec{r}), \lambda_i)) \tag{2.1}$$

with N, the number of launched rays.

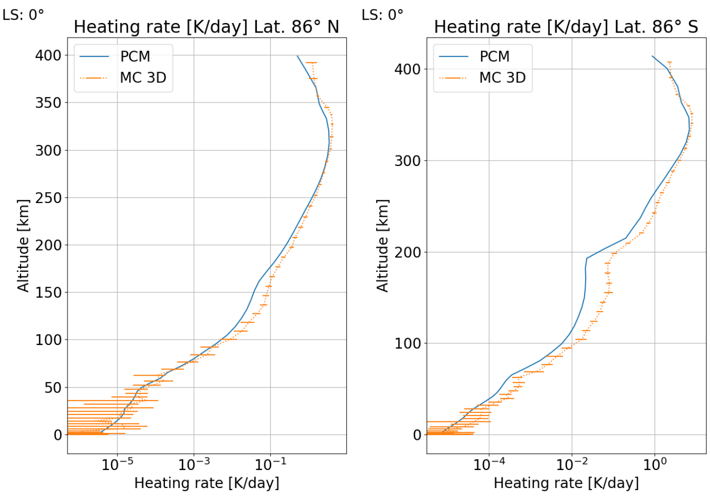

Fig. 2. Left: Heating rates at north pole. **Right:** Heating rates at south pole. The solid lines are the 2-stream results and the dotted lines are the 3D Monte Carlo model results.

3 Results

In this section, we explore the results obtained with the Monte Carlo model for two cases: at northern spring equinoxe ($L_S = 0°$) and at southern winter solstice ($L_S = 90°$). In both cases, we run the calculations on a slice of atmosphere composed of 47 columns from the north pole to the south pole, at a fixed longitude choosen as the sub-solar longitude.

3.1 Northern spring equinoxe

For the equinoxe scenario, the sub-solar latitude is set to 0°N. Fig. 1 presents the heating rates dependence with the altitude and latitude. We observe a rather good agreement between the Monte Carlo and the 2-stream, with similar structures, though differences appear. As shown by Fig. 2, the models diverge between 100 and 200 km near the poles, where the Monte Carlo model provides larger heating rates, linked to sphericity effects. Interestingly, we observe an assymetry between the poles, with the difference between the models being more important at the south pole. This is related to heterogeneity effects. Indeed, as can be observed in Fig. 3, an opaque region produced by a patch of fractal aggregates is present at the south pole between 200 and 300 km and for latitudes comprised between 70°S and 90°S. In a plane-parallel model, such a feature decreases the heating rates below the opaque haze patch as it blocks most of the incoming radiation. However, in a 3D model, in addition to the scattered light, a direct contribution from the source coming from the side can reach the region below the opaque haze patch whitout the necessity of crossing this region. This results in larger heating rates below the haze patch in the 3D model.

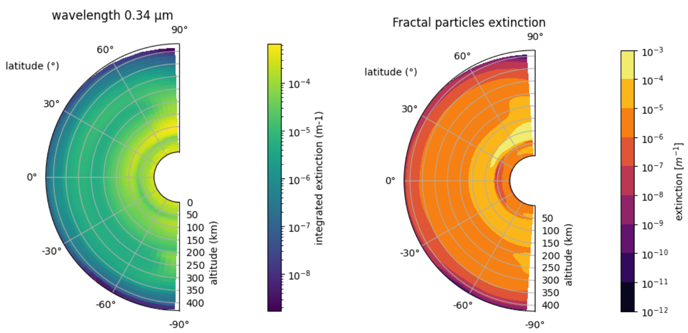

Fig. 3. Left: Polar plots of the extinction coefficient at 0.34 μm **Right:** Polar plots of the extinction by fractal aggregates.

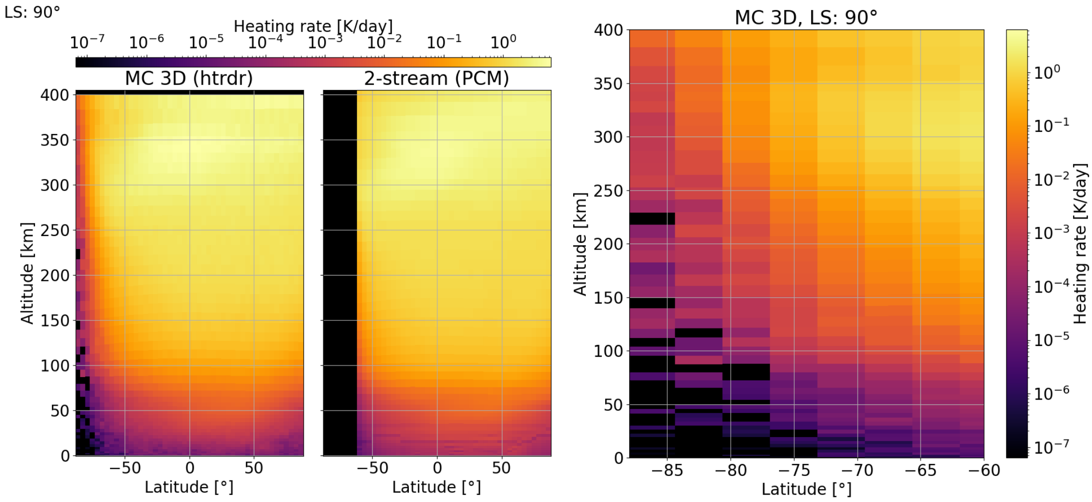

Fig. 4. Heating rates along altitude and latitude, in Titan atmosphere, at southern winter solstice ($L_S = 90°$), using Titan PCM optical properties. **Left:** Comparison between the 3D Monte Carlo model and the 2-stream model of the Titan PCM. **Right:** Zoom in the polar night of the Monte Carlo results.

3.2 *Southern winter solstice*

The heating rates obtained in the solstice scenario are presented in Fig. 4. What is most stricking is the absence of data in the whole polar region for the 2-stream model, even at high altitude. This is a limitation of the plane-parallel model that cannot account for a source with an incidence angle larger than 90°. Nevertheless, light can reach this region. First, direct light from the sun can reach the pole above 300 km and even below for columns at lower latitudes. Therefore, most of the polar region actually receives a direct contribution from the sun and therefore presents strong heating rates comparable with those found outside the polar region (right panel of Fig 4). In addition, a scattered contribution can affect even the deep region of the polar night.

4 Conclusions

Thanks to the use of a 3D Monte Carlo radiative transfer code, we have quantified the impact of heterogeneities (like patches of haze or clouds) on the radiative transfer and local budget in Titan's atmosphere. The heating rates obtained in the polar night are strong and it is of capital importance to correctly account for the radiative budget in this region. The use of a 3D model as htrdr-planets coupled to the Titan PCM appears to be primordial in order to correctly simulate the radiative bugdet in this atmosphere and the physical processes affected.

This work is supported by the Agence National de la Recherche (ANR) through the RaD3-net project (ANR-21-CE49-0020-01). We thank the organizers of the SF2A 2025.

References

de Batz de Trenquelléon, B., Rannou, P., Burgalat, J., Lebonnois, S., & d'Ollone, J. V. 2025a, The Planetary Science Journal, 6, 79

de Batz de Trenquelléon, B., Rosset, L., d'Ollone, J. V., et al. 2025b, The Planetary Science Journal, 6, 78

He, Z., Vinatier, S., Eymet, V., et al. submitted

Hourdin, F., Talagrand, O., Sadourny, R., et al. 1995, Icarus, 117, 358

Lebonnois, S., Burgalat, J., Rannou, P., & Charnay, B. 2012, Icarus, 218, 707

Lora, J. M., Lunine, J. I., & Russell, J. L. 2015, Icarus, 250, 516

Villefranque, N., Fournier, R., Couvreux, F., et al. 2019, Journal of Advances in Modeling Earth Systems, 11, 2449